MULTIPLE COMPTON SCATTERING

By

William R. Faust

Thesis submitted to the Faculty of the Graduate School
Of the University of Maryland in partial
fulfillment of the requirements for the
degree of Doctor of Philosophy

June, 1949

ACKNOWLEDGMENT

The author wishes to express his appreciation to Dr. M.H. Johnson for suggesting this problem and for his active interest and guidance in the completion of the research.

W.R.F.

TABLE OF CONTENTS

LIST OF TABLES

LIST OF FIGURES

SECTION I

INTRODUCTION

Extensive data on scattering[1] of x rays and gamma rays has indicated that the Klein-Nishima formula[2] is reliable up to energies[3] of about 5 mc^2. Most of these data have been total cross-section measurements. The angular distribution of scattered quanta has been measured[4] also and compares favorably with the Klein-Nishma distribution. Recent data[5] give some indication that the Klein-Nishima formula probably is correct even up to energies of 30 mc^2. In any event, it will be assumed to hold correctly in this application.

---

[1] A.H. Compton and S.K. Allison, X Rays in Theory and Experiment (New York, D. Van Nostrand, 1935), Chap. III, pp. 116-262.

[2] O. Klein and Y. Nishima, "Uber die Streuung Von Strahlung durch freie Electronen nach der neuen relativistichen Quantemdynamik Von Dirac", Zeitschrieft fur Physik, 52: 853-868, May 1929.

[3] L. Meitner and H. Upfeld, "Uber das Absorptionsgesetz fur Kurzwellige -struhlung", Zs. f. Phys., 67: 147-168, February, 1931.

[4] G.E.M. Jauncy and G.G. Harry, "The Scattering of Unpolarized X Rays", Physical Review, 37: 698-711, May, 1931.

[5] G.D. Adams, "Absorption of High Energy Quanta", Physical Review, 74: 1702-1712, October, 1948.

In spite of the large amount of data collected on scattering, there has been a failure to emphasize multiple scattering. Since the total intensity of a gamma-ray beam is composed of primary and scattered radiation, a knowledge of the multiple process is prerequisite to an accurate description of the transmission of radiation through matter. Some recent papers have dealt with the analysis of multiple scattering, one[6] of which considered in an approximate manner the intensity due to multiple scattering of a relatively soft x-ray beam. The other[7] calculated a component of the intensity of a plain parallel gamma-ray beam incident upon a thick target. Results of the latter are difficult to interpret and compare with experimental measurements. Another paper[8] calculated the intensity due to a plane source but considered only isotropic scattering.

The geometrical factors introduced by a beam generally make the results difficult to analyze. An essential simplification is possible by elimination of the geometrical factors entirely. This can be done by the use of a gamma-ray source homogeneously distributed throughout an infinite

---

[6] L.F. Lamerton, "Theoretical Study of Results of Ionization Measurements in Water with X Rays and Gamma Rays", British Journal of Radiology, 1: 246, June, 1948.

[7] J.O. Hirschfelder, J.L. Magee, and M.H. Hull, Physical Review, 73: 852-868, April 15, 1948.

[8] S. Chandrasekhar, "The Softening of Radiation by Multiple Compton Scattering", Proceedings of the Royal Society, 192: 508-518, March 18, 1948.

volume. multiple scattering effects then manifest themselves in the intensity and spectral distribution of the radiation, which is the same at every point in the medium. By considering multiple scattering as a succession of steps which are the same for every emitted gamma ray, the spectral distribution and absolute magnitude of the intensity can be calculated. Such an experiment[9] has been carried out at the Naval Research Laboratory. Agreement of the calculated intensity with the observed was excellent.

In order to extend the methods, experiments have been performed in which the total radiation intensity was dependent upon a single parameter, i.e., the distance from a source. These experiments which constitute the topic of this thesis consisted essentially of measuring the intensity as a function of the distance from a radiating point and a radiating plane immersed in an unbounded medium.

---

[9] W.R. Faust and M.H. Johnson, "Multiple Compton Scattering", Phy. Rev., 75: 467-472, February, 1949.

SECTION II

THEORY

Part 1. Interaction between matter and radiation modifies characteristics of the radiation as it travels through the medium. Two general classes of such interation are absorption and scattering. A quantitative description of these processes makes use of the "cross-section", which is defined as

$$\sigma = \frac{\text{Number of processes occurring per second.}}{\text{Incident flux of radiation}}$$

Absorption processes[10] are those in which a primary quantum disappears producing simultaneous changes in the physical state of the matter. The three main absorption processes are excitation of an atom by light, photoelectric effect, and pair production.

The first process is a resonant one in which a quantum is absorbed by a bound electron with a simultaneous transition of the electron to a higher energy state. Photoelectric effect[11] is similar to the above absorption process with the exception that the final state of the electron lies in the region of continuous energy elevels. The electron is

[10] W. Heitler, Quantum Theory of Radiation (Oxford, Cambridge, 1944) pp. 129-137.

[11] H.R. Hulme, J. McDougall, R.A. Buckingham, R.H. Fowler, "The Photoelectric Absorption of Rays in Heavy Elements", Proceedings of the Royal Society, 194: 131-151, January, 1935.

ejected from the atom with an energy equal to the difference between the quantum energy and the ionization energy of the atom. This process leads to continuous absorption and decreases rapidly for energies well above the K absorption limit of the atom. Pair production[12] refers to the absorption of a quantum of energy greater than 2 mc^2 and the simultaneous creation of a positive and a negative electron in the field of the nucleus. A formal description of this process is the same as the photoelectric effect except that the electron is initially in a negative energy state. Absorption of the quantum raises this electron to a state of positive energy where it is observable as an ordinary electron while the "hole" left in the negative energy states acts as a positive electron.

Scattering processes are those in which a primary quantum is absorbed with the simultaneous emission of a secondary quantum. According to the quantum theory of radiation, the energy of a scattered quantum is $E^1 = E + (E_1 - E_k)$ where E_1, E_k are energy levels of two atomic states, and E is the energy of the incident quantum. If $E_1 - E_k = 0$, the scattered radiation is usually coherent with the primary radiation and has a distribution identical with the classical or

---

[12] J.R. Oppenheimer and M.S. Plesset, "On the Production of the Positive Electron", Phy. Rev., 44: 53-55, January, 1933.

Thompson distribution. If $E_1 - E_k \neq 0$, the Raman or Smekalal lines are re-emitted, the scattered light having either an increased or decreased frequency.

For high energy quanta, these processes are unimportant as electrons act as though they were free. Interaction between light and free electrons is called Compton scattering. From conservation laws, the energy E^1 of a scattered quantum is

$$E^1 = \frac{E}{1 + \frac{E}{mc^2}(1 - \cos\theta)} \tag{1}$$

where θ is the angle of scattering. Klein and Nishima[13] give the cross-section for this process as

$$\frac{\sigma}{\sigma_0} = \frac{3}{4}\left\{\frac{1+\alpha}{\alpha^3}\left[\frac{2\alpha(1+\alpha)}{1+2\alpha} - \ln(1+2\alpha)\right] + \frac{1}{2\alpha}\ln(1+2\alpha) - \frac{1+3\alpha}{(1+2\alpha)^2}\right\} \tag{2}$$

Here $\sigma_0 = \frac{8\pi}{3} r_0^2$ is the Thompson cross-section and $r_0 = e^2/mc^2$ is the classical electron radius. α is the energy in units of mc^2.

It is not necessary to consider all the above-mentioned processes in a theoretical description of the experiments. These experiments were performed in water with quanta of 1.20 Mev initial energy, and measurements made by means of a detector which was responsive only to energies greater than .08 Mev. Pair production is negligible relative to Compton scattering since it starts at 1.02 Mev and has a cross-section equal to the Compton cross-section in

---

[13] O. Klein and Y. Nishima, loc. cit.

water at 30 Mev. Photoelectric effect is also negligible relative to Compton scattering since photoelectric cross-section in water is equal to Compton at about .025 Mev and decreases as the energy is increased. Other processes mentioned occur at energies comparable with the ionization energy of the atoms and do not lead to continuous absorption.

Part 2. A quantum traveling through a medium is scattered successively, losing energy at each scattering according to Equation (1). Since the differential cross-section is energy dependent, general characteristics of the quantum's path change from point to point. Initially, when it has a high energy, according to the Klein-Nishima formula, the quantum has a greater probability of scattering in the forward direction than in the backward direction. Furthermore, the distance (mean free path) between the scatterings is relatively long. As the energy is reduced by successive scatterings, the mean free path decreases, and the probability of scatter is about equal in the forward and backward directions. Finally, its energy is degraded to a sufficiently low value that it is absorbed photoelectrically.

To describe the multiple scattering process and relate the counting rate to the source strength, properties of the medium and of the detector, the quanta are divided into groups determined by the number of scatterings experienced, i.e., the k-th group is scattered k times. A quantum traveling through the medium is scattered successively losing energy in accordance with the Compton formula. Since the range of angles through which a quantum is scattered is determined by probability, the quanta of a particular group do not have the same energy but have energies distributed about a mean energy E_k.

The mean energy scattered per second by an electron can be obtained by integration of the Klein-Nishima expression for intensity[14] over a spherical surface. If this result is divided by the product σI, of the total Klein-Nishima cross-section and the incident intensity, the resulting ratio, σ_s/σ, is the fraction of the incident energy given to a scattered quantum,

$$\frac{\sigma_s}{\sigma} = \frac{\frac{2\alpha}{(1+2\alpha)^2} + \frac{4\alpha}{3(1+2\alpha)^2} + \frac{1}{3\alpha^2}\left[\mathrm{Ln}(1+2\alpha) - \frac{2\alpha(1+3\alpha)}{(1+2\alpha)^3}\right]}{\frac{1+\alpha}{\alpha^3}\left[\frac{2\alpha(1+\alpha)}{1+2\alpha} - \mathrm{Ln}(1+2\alpha)\right] + \frac{1}{2\alpha}\mathrm{Ln}(1+2\alpha) - \frac{1+3\alpha}{(1+2\alpha)^2}} \qquad (3)$$

where $\alpha = E/mc^2$. This ratio is plotted in Figure 1 as a function of energy.

It is now assumed that each quantum passes through a succession of energy values given by the mean energy of the various groups[15] so that the actual problem is replaced by one in which all quanta of the k-th group have the mean

---

[14] W. Heitler, loc. cit.

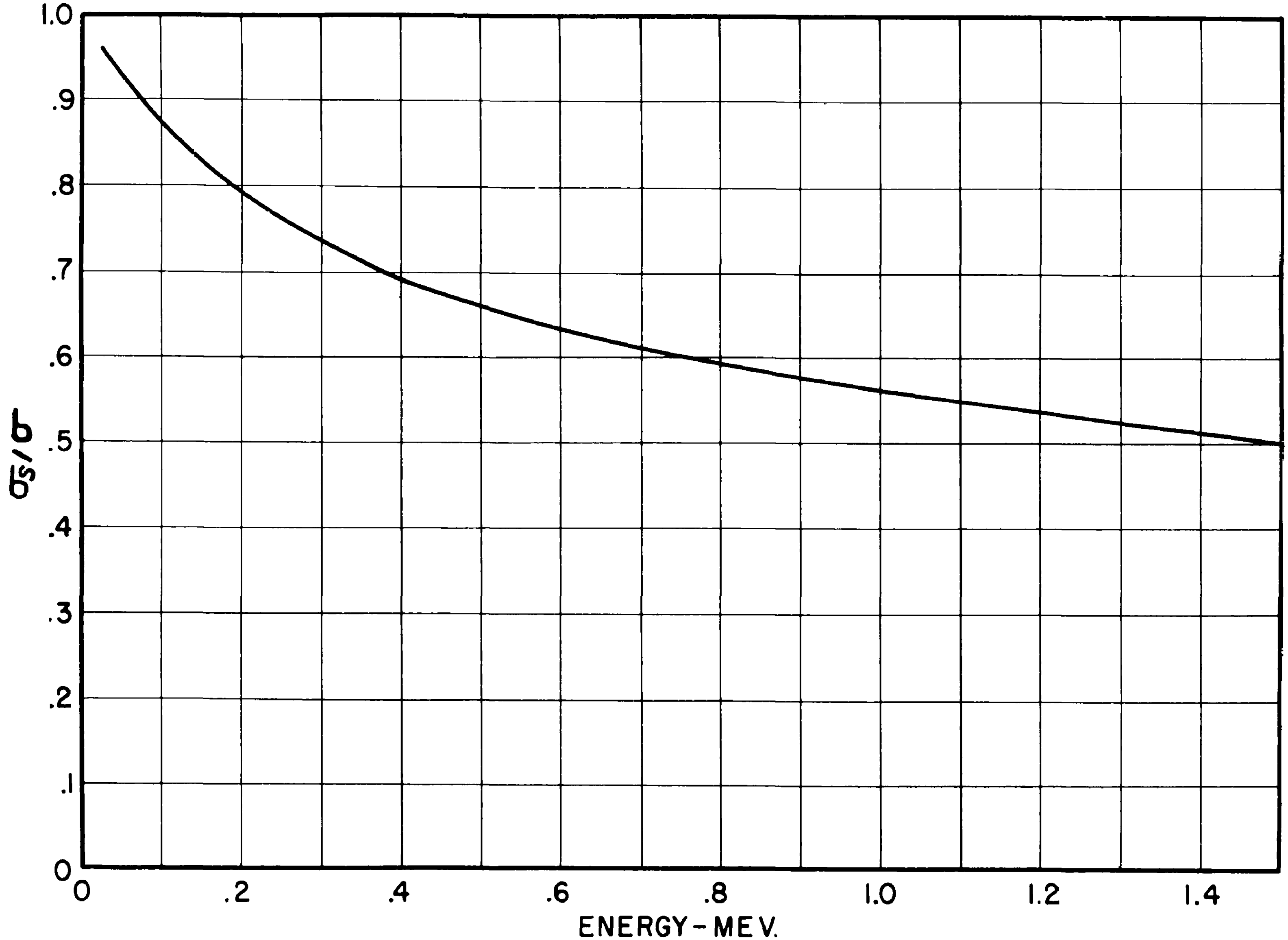

Figure 1. Ratio of Scattered to Incident Energy.

energy E_k. With this assumption, the mean energy of the k-th group is

$$E_K = (\sigma_s/\sigma)\ E_{K-1} \tag{4}$$

where (σ_s/σ) is evaluated at the energy E_{k-1}. The succession of energy values assumed by the various groups[15] is given in Table I for an initial energy of 1.20 Mev.

<u>Part 3</u>. A theory describing exact spectral and spatial distribution of quanta due to a point source can be formulated in a manner analagous to that followed by Hopf[16]. Let $I(\cos\theta, \rho, \lambda)\,d\Omega\,d\lambda$ be the number of quanta per unit volume at ρ cm from the source, in the wave length interval $d\lambda$ and making angle θ relative to ρ, such that they are moving in the solid angle $d\Omega$. Then the differential equation governing I is

$$\cos\theta\frac{\partial I}{\partial\rho} - \sin\theta\frac{\partial I}{\rho\,\partial\theta} + N\sigma I = N\int_0^{2\pi} d\phi' \int_0^{\pi} I\left(\cos\theta', \rho, \lambda - \frac{h}{mc}(1-\cos|\Theta|)\right) f\left(\cos|\Theta|, \lambda - \frac{h}{mc}(1-\cos|\Theta|)\right)\sin\theta'\,d\theta'$$

Here $f\left(\cos|\Theta|, \lambda - \frac{h}{mc}(1-\cos|\Theta|)\right)$ is the differential Compton cross-section, and N is the electron density. $|\Theta|$ is the angle between the directions specified by (θ, ϕ) and (θ', ϕ'). Unfor-

---

[15] Faust and Johnson, <u>loc. cit.</u>

[16] E. Hopf, <u>Problems of Radiative Equilibrium</u> (Oxford, Cambridge, 1932) pp. 2-12.

TABLE I

SCATTERED ENERGIES AND LINEAR ABSORPTION COEFFICIENTS

E Mev	σ_s/σ	μ cm^{-1}	μ^+ cm^{-1}	μ^- cm^{-1}
1.20	.545	.0643	.0475	.0174
.654	.63	.0861	.0603	.0246
.412	.69	.102	.0705	.0341
.284	.73	.1178	.0784	.0341
.207	.79	.1333	.0850	.0524
.064	.825	.134	.0894	.0574
.135	.845	.135	.0925	.0634
.113	.86	.113		
.098	.875	.098		
.086	.89	.086		

tunately it is possible to obtain solutions of this equation only for isotropic scattering.[17] Therefore, in order to obtain a description of a radiating point source, the problem will be attacked from a different point of view.

As in Part 2, the actual problem will be replaced by one in which all quanta of group k have the mean energy E_k, where E_k is given by Equation (2). Let $F_k(\rho) = F_k^+ + F_k^-$ be the total number of quanta per second of group k passing through a sphere of radius ρ, about the point source. F_k^+/F_k is the fraction with angles θ relative to the radius vector between zero and $\pi/2$ and F_k^-/F_k is the fraction with $\pi/2 \leq \theta \leq \pi$.

σ, the cross-section can also be decomposed in a similar manner, i.e., $\sigma = \sigma^+ + \sigma^-$ where σ^+/σ is the fraction of incident quanta scattered into directions with $0 \leq \theta \leq \pi/2$ and σ^-/σ is the fraction scattered in to $\pi/2 \leq \theta \leq \pi$. σ^+ is obtained by integration of the differential cross-section between 0 and $\pi/2$ while the integration is between $\pi/2$ and π for σ^-. Expressions for these qualities are

$$\frac{\sigma^+}{\sigma_0} = \frac{3}{4}\left\{\frac{1+\alpha}{\alpha^3}\left[\alpha - \ln(1+\alpha)\right] + \frac{1}{2\alpha}\ln(1+\alpha) - \frac{2(1+\alpha)^2 + \alpha^2}{(1+\alpha)^2} \right. \tag{5}$$

$$\frac{\sigma^-}{\sigma_0} = \frac{\sigma}{\sigma_0} - \frac{\sigma^+}{\sigma_0} \tag{6}$$

[17] S. Chandrasekhar, <u>loc. cit.</u>

It will be assumed that the contribution to the positive component of group k from group k-1 scattered in the spherical shell between ρ and $\rho + \delta\rho$ is

$$N\sigma F^+_{k-1}\,\delta\rho\left(\frac{\sigma^+_{k-1}}{\sigma_{k-1}}\right) + N\sigma F^-_{k-1}\,\delta\rho\left(\frac{\sigma^-_{k-1}}{\sigma_{k-1}}\right) \tag{7}$$

The first term is the fraction scattered into the positive direction from F_{k-1} while the last is the contribution to the positive component from F_{k-1}. This formulation is not entirely correct as it assumes that quanta traversing the spherical shell travel the same distance. Actually those quanta in a small range of angles about θ, travel a distance $\delta\rho/\cos\theta$. A still more serious difficulty is the assumption that $N\sigma\,\delta\rho\, F^+_{k-1}\left(\frac{\sigma^+}{\sigma}\right)$ represents the outward scattered quanta. Actually quanta traversing the spherical shell in a solid angle $d\Omega$ about θ, will be scattered so that some will be scattered inward also. This should be clear from the illustration of Figure 2. Similar remarks also apply to the negative traveling quanta. In spite of these objections, expression 7 will be used in the following calculation. Then the positive component of group k crossing a sphere of radius $\rho + \delta\rho$ is

$$F^+_k(\rho+\delta\rho) = F^+_k(\rho) - N\sigma F^+_k(\rho)\,\delta\rho + N\,\delta\rho\left(\sigma^+_{k-1}F^+_{k-1}(\rho) + \sigma^-_{k-1}F^-_{k-1}(\rho)\right) \tag{8}$$

where $N\sigma\,\delta\rho\, F^+_k$ is the quanta scattered out of group k. If terms of order $(\delta\rho)^2$ are neglected, then,

$$\frac{\partial F^+_k}{\partial\rho} + N\sigma F^+_k = N\left(\sigma^+_{k-1}F^+_{k-1} + \sigma^-_{k-1}F^-_{k-1}\right) \tag{9}$$

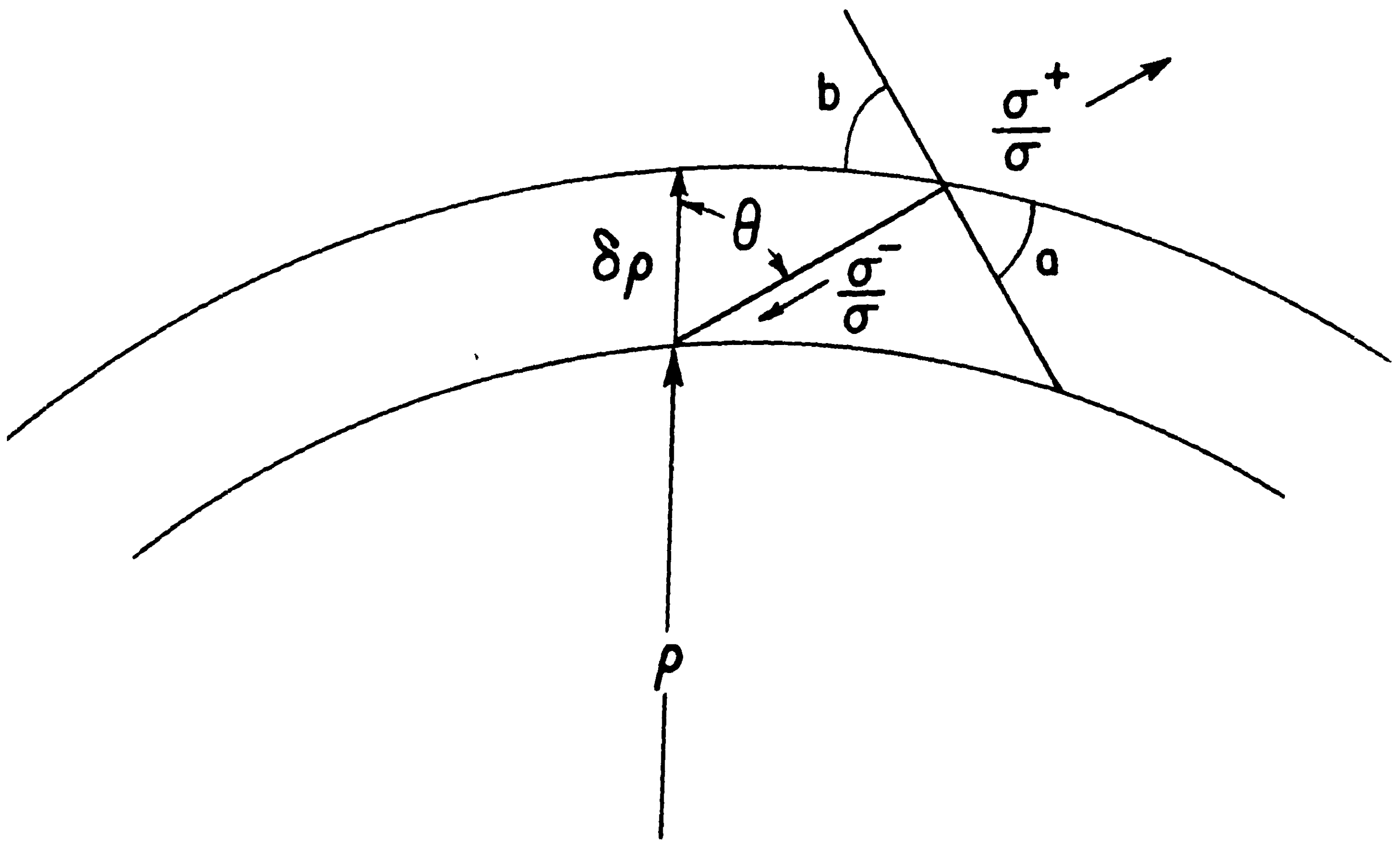

Figure 2. Errors in Assumed Form of Scattering.
a. Angle a is proportional to quanta actually scattered inward from $\sigma^+_{K-1}F^+_{K-1}\delta\rho$
b. Angle b is proportional to quanta actually scattered outward from $\sigma^-_{K-1}F^-_{K-1}\delta\rho$

In a similar manner it can be shown that

$$-\frac{\partial F_K^-}{\partial \rho} + N\sigma F_K^- = N\left(\sigma_{K-1}^- F_{K-1}^+ + \sigma_{K-1}^+ F_{K-1}^-\right) \qquad (10)$$

Particular solutions of equations (9) and (10) that vanish exponentially at large distances and give $F_k^+(0) = 0$ and $F_k^-(0)$ = finite, as is expected physically are

$$F_K^+ = e^{-\mu_K Z}\int_0^Z e^{\mu_K \rho}\left(\mu_{K-1}^+ F_{K-1}^+ + \mu_{K-1}^- F_{K-1}^-\right)d\rho \qquad (11)$$

$$F_K^- = e^{\mu_K Z}\int_Z^{\infty} e^{-\mu_K \rho}\left(\mu_{K-1}^- F_{K-1}^+ + \mu_{K-1}^+ F_{K-1}^-\right)d\rho \qquad (12)$$

where for brevity $\mu_K^+ = N\sigma_K^+$ etc. μ_K^+ and μ^- were computed from Equations (5) and (6) and are plotted as a function of energy in Figure 3. μ_K was calculated from Equation (2) and is given in Table I.

Evidently the only physical solutions of equations (7) and (8) for the zero group are $F_0^+ = n\lambda e^{-\mu_0 Z}$, $F_0^- = 0$, where $n\lambda$ is the number of quanta of energy E_0, emitted per second by the source. Equations (11) and (12) then can be solved successively and are given in Appendix I up to Group 4. For groups or orders greater than 4, the integrations were performed numerically, and results are given in Table II.

Since $(F_k^+ + F_k^-)$ is the total number of quanta of group k passing through a sphere of radius Z, the number crossing unit area is $(F_k^+ + F_k^-)/4\pi Z^2$. Therefore, a Geiger counter of effective area A and efficiency ϵ will register counts

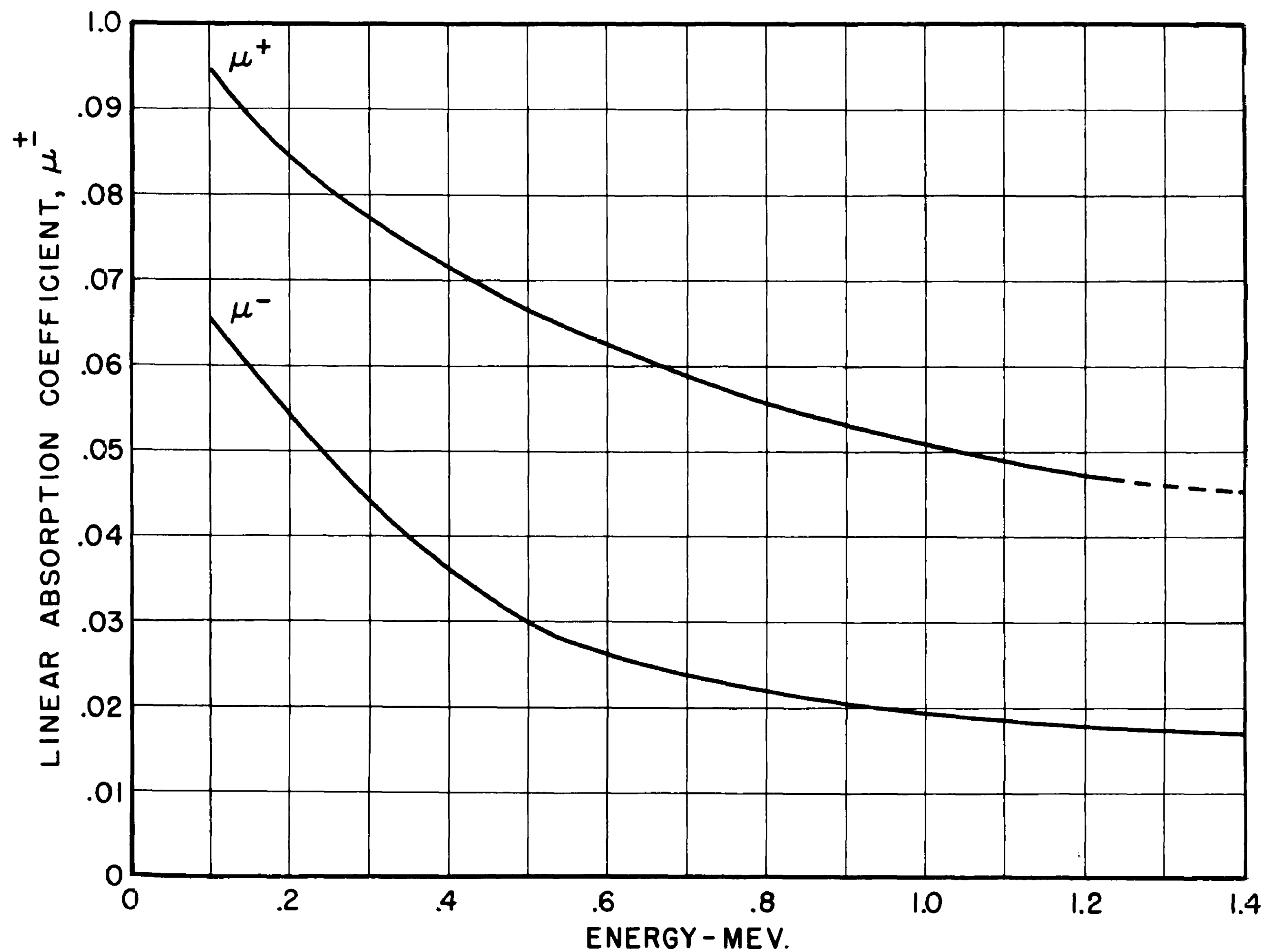

Figure 3. Directional Absorption Coefficients.

TABLE II

DISTRIBUTION FUNCTIONS FOR A UNIT POINT SOURCE EMITTING 1.20 MEV QUANTA

Z cm	F_0^+ NO/S.	F_1^+ NO/S.	F_2^+ NO./S.	F_3^+ NO/S.	F_4^+ NO/S.	F_5^+ NO/S.	F_6^+ NO/S.	F_7^+ NO/S.	F_8^+ NO./S.
0	1.000	0.000	0.00	0.00	0.000	0.00	0.00	0.00	0.00
10	.5257	.2250	.0719	.0295	.0247	.0187	.0164	.0144	.0130
20	.2763	.2120	.1201	.0750	.0560	.0456	.0335	.0282	.0260
30	.1454	.1520	.1134	.0815	.0677	.0511	0411	.043	.035
40	.0765	.0977	.0907	.0803	.0687	.0588	.0531	.042	.038
50	.0404	.0562	.0605	.0542	.0454	.0452	.0437	.041	.036
60	.0213	.0387	.0467	.0377	.0343	.0344	.0337	.031	.026
70	.0111	.0192	.0235	.0247	.0240	.0233	.0233	023	.022
80	.0059	.0105	.0129	.0149	.0148	.0152	.0156	.0157	.0158
90	0031	.0058	.0078	.0091	.0100	.0097	.0101	.0105	.0106
100	.0016	.0031	.0045	.0053	0055	.0057	.0063	.0066	.0070

Z cm	F_0^- NO/S.	F_1^- NO/S.	F_2^- NO/S.	F_3^- NO/S.	F_4^- NO/S.	F_5^- NO/S.	F_6^- No./S.	F_7^- No./S.	F_8^- No/S
0	0.00	.1157	.0789	.0544	.0411	.0314	.0265	.0242	.019
10	0.00	.0607	.0708	.0610	.0489	.045	.0365	.0349	.031
20	0.00	.0320	.0493	.0534	.0501	.049	.047	.040	.037
30	0.00	.0168	.0312	.0397	.0411	.0493	.0487	.045	.041
40	0.00	.0089	.0167	.0274	.0322	0470	0359	034	.030
50	0.00	.0047	.0108	.0169	.0230	.0237	.0244	.027	.024
60	0.00	.0027	.0069	.0113	.0133	.0163	.0175	.018	.018
70	0.00	00129	0034	.0060	.0090	.0095	.0111	.012	.0127
80	0.00	.00068	.0019	0034	.0048	.0058	0071	.0070	.0072
90	0.00	.00036	.00099	.0019	.0260	.0038	0044	.0051	.0049
100	0.00	.00019	.00053	0011	.0015	.0026	.0028	.0032	.0030

due to all groups at a rate

$$R = \frac{A}{4\pi Z^2} \sum_{\kappa=0}^{\kappa=\infty} (F_\kappa^+ + F_\kappa^-)\, \epsilon_\kappa \tag{13}$$

A is the counter area projected in a plane perpendicular to the radius vector.

If the counter characteristics are modified by means of a directional shield which has transmission coefficients T_k^+ and T_k^- in the positive and negative directions respectively, the counter efficiency is reduced at each energy by just these coefficients so that the shielded counting rate is

$$R = \frac{A}{4\pi Z^2} \sum_{\kappa=0}^{\kappa=\infty} (T_\kappa^+ F_\kappa^+ + T_\kappa^- F_\kappa^-)\, \epsilon_\kappa \tag{14}$$

The $T_k^{\pm}$ are computed from the known mass absorption coefficients.[18]

Since photoelectric absorption in the detector walls causes the detector response to vanish at some energy E_p, the infinte sums in Equation (13) and (14) may be replaced by sums extending from zero to p, where p corresponds to the detector cut-off energy. This energy can be estimated from the transmission curve of the counter walls. E_p is the energy corresponding to $T = 0.50$.

[18] Compton, l.c. cit.

Part 4. It is expedient to consider a plane source as a distribution of unit point sources of density $n\lambda$ over a surface "S". The number of quanta of group k incident per second upon a cylindrical counter of unit projected area placed as in Figure 2, is

$$I_k = \int_0^{2\pi} \int_0^{\pi} (F_k^+ + F_k^-) \frac{\sqrt{\cos^2\theta + \sin^2\theta \sin^2\varphi}}{4\pi\rho^2} \rho^2 \tan\theta \, d\theta \, d\varphi \qquad (15)$$

Here θ is the polar angle measured from the negative Z direction, and φ is the longitude measured from the counter axis. The factor $\sqrt{\cos^2\theta + \sin^2\theta \sin^2\varphi}/\rho^2$ is the solid angle subtended by the counter at a distance ρ from an element of the plane source. By an obvious transformation and integration over φ, this expression can be written as

$$I_k = \frac{1}{\pi} \int_Z^{\infty} (F_k^+ + F_k^-) \; E(\cos^{-1} Z/\rho, \pi/2) \; d\rho \qquad (16)$$

where $E(\cos^{-1} Z/\rho, \pi/2)$ is the complete elliptic integral of the second kind. Direct calculation with the aid of table of functions[19] shows that[20]

$$I_k = \frac{1}{2} \int_Z^{\infty} \frac{(F_k^+ + F_k^-)}{\rho} \, d\rho \qquad (17)$$

is a good approximation to equation (16) and is accurate

---

[19] Eugene Jahnke and Fritz Emde, Tables of Functions, (New York, Dover Publications, 1945) pp.6-9.

[20] Equation (17) is exact for a spherical counter. Actually, the response should be somewhere between equations (16) and (17).

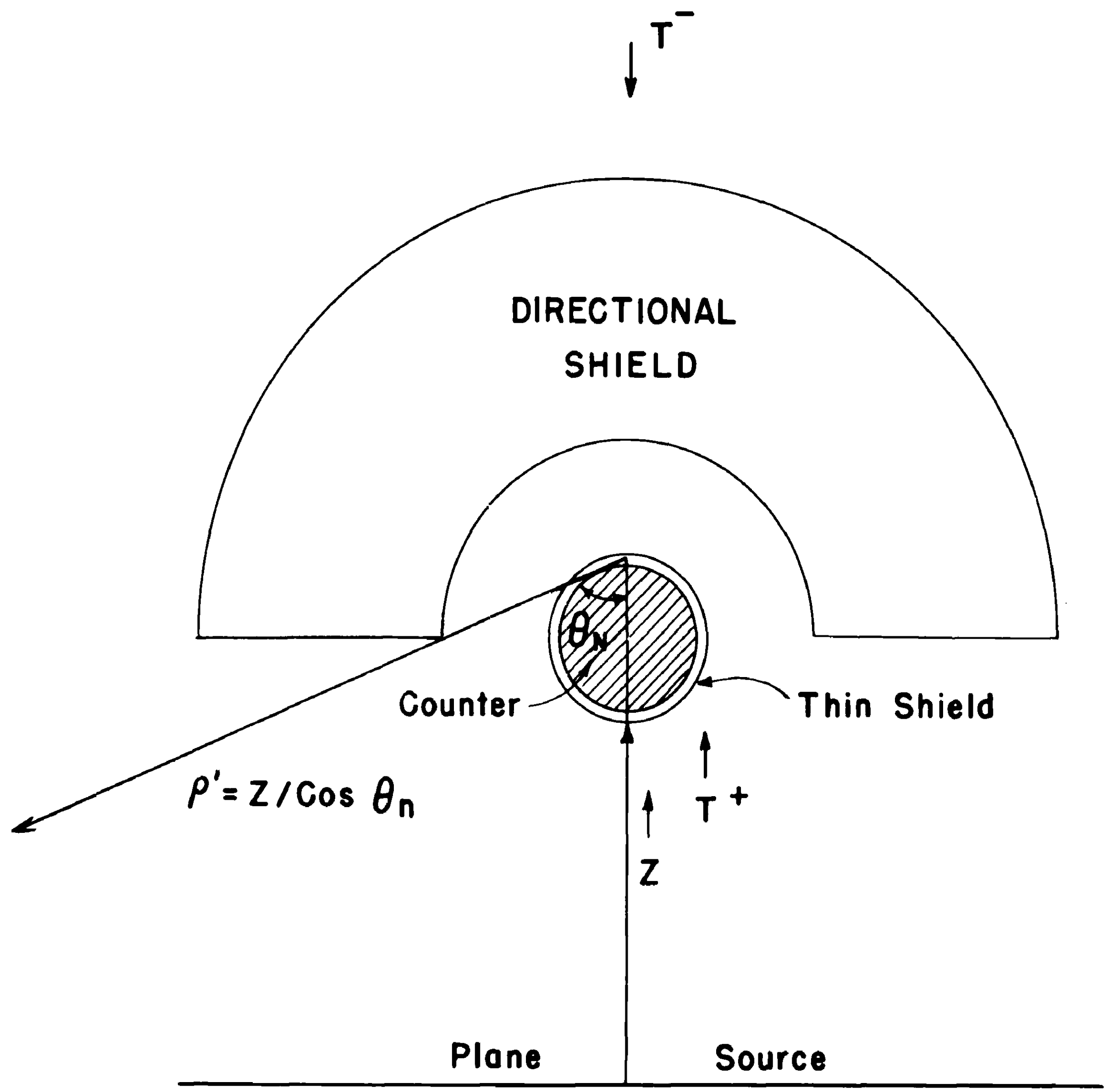

Figure 4. Cylindrical Counter and Shields.

within two per cent for $Z \geqslant 20$.

Analogous to the description of the point source, the shielded counting rate for a counter of area A is

$$R = A \sum_{k=0}^{k=p} \epsilon_K I_K T_K \tag{18}$$

where T_k is the transmission coefficient of a thin shield completely surrounding the counter.

Introduction of a directional shield as shown in Figure 4 separates the radiation into components moving toward and away from the source. The number of outward traveling quanta incident per second upon a cylindrical counter of unit area is

$$I_K = \frac{1}{\pi}\int_Z^{Z/\cos\theta_n} \frac{F_K^+}{\rho} E(\cos^{-1} Z/\rho, \pi/2)\, d\rho + \frac{(1+T_K)}{2\pi}\int_{Z/\cos\theta_n}^{\infty} \frac{F_K^+}{\rho}\, d\rho \tag{19}$$

Since $\theta_n \approx 70^\circ$, this expression is approximately

$$I_k = \frac{1}{2}\int_Z^{\infty} \frac{F_K^+}{\rho}\, d\rho \tag{20}$$

In a similar manner the quanta incident upon the counter from the negative direction can be represented by

$$I_k^- = \frac{1}{2}\int_Z^{\infty} \frac{F_K^-}{\rho}\, d\rho \tag{21}$$

These functions are given in Table III.

The total counting rate for a counter of area A is

$$R = A \sum_{k=0}^{k=p} \epsilon_K (T_K^+ I_K^+ + T_K^+ I_K) \tag{22}$$

TABLE III

DISTRIBUTION OF 1.20 MEV. QUANTA DUE TO A PLANE SOURCE EMITTING ONE QUANTUM PER cm^2 PER SECOND

Z cm	I_0 NO/cm^2/S	I_1^+ NO/cm^2/S.	I_2^+ NO/cm^2/S.	I_3^+ NO/cm^2/S	I_4^+ NO/cm^2/S	I_5^+ NO/cm^2/S	I_6^+ NO/cm^2/S	I_7^+ NO/cm^2/S	I_8^+ NO/cm^2/S
0	∞	.151	.135	-	-	-	-	-	-
10	.220	.153	.093	.065	053	.041	.038	.034	.030
20	.068	.073	.056	.042	.036	0311	.029	.027	.024
30	.027	.034	.031	.026	.024	.022	.0214	.019	.015
40	.0135	.0164	.0173	.015	.0145	.0143	.0142	.0136	.013
50	.0049	.0079	.0095	.0090	.0087	.0086	.0088	0091	0091
60	.0025	.0037	.0048	.0052	.0050	.0051	.0052	.0052	.0051
70	.00105	.0019	.0025	.0027	.0027	.0029	.0029	.0031	.003
80	.0005	.0087	.0013	.00155	.00143	.0017	.0017	.00179	.0018
90	.00025	.0045	.00065	.00079	.0071	.00095	.0009	.00099	001
100	.00011	.00022	.00032	.00036	.00038	.00040	.00048	.00055	.0005

Z cm	I_0^- NO/cm^2/S	I_1^- NO/cm^2/S	I_2^- NO/cm^2/S	I_3^- NO/cm^2/S	I_4^- NO/cm^2/S	I_5^- NO/cm^2/S	I_6^- NO/cm^2/S	I_7^- NO/cm^2/S	I_8^- NO/cm^2/S.
0	0.00	∞	∞	∞	∞	∞	∞	∞	∞
10	0.00	.0243	.035	.0398	.050	.041	.038	.0355	.032
20	0.00	.0066	.0149	.0193	.020	.0243	.0243	.0225	.022
30	0.00	.0034	.0065	.0094	.0107	.0144	.0137	.0139	.0014
40	0.00	.0013	.0030	.0048	.0059	.0078	.0077	.0082	.0088
50	0.00	.00057	.0014	.0024	0028	.0041	.0043	.0047	.0051
60	0.00	.00026	.00066	.0012	0017	.0022	.0025	.0027	.0029
70	0.00	.00012	.00033	.00063	.00089	.0012	.0014	.0015	.00165
80	0.00	.000058	.0016	.00034	.00048	.00068	.00077	.00085	.00096
90	0.00	.000027	.000078	.00015	.00024	.00038	.00043	.00049	.00057
100	0.00	.000013	.000037	.000088	.000117	.00022	.00024	.00028	.00032

where T_k^+, T_k^- are respectively the transmission coefficients of a directional shield parallel and anti-parallel to the Z axis.

SECTION III

DESCRIPTION OF EXPERIMENTS

Experiments approximating those described may be performed in a large volume of water and measurements proportional to the intensity made with a Geiger-Muller counter. Sources of finite size must be used instead of the idealization of point and infinite plane sources. Restrictions on the validity of such approximations require that intensity determinations cannot be made at extremities (within a mean free path) of the volume and, furthermore, that in case of the plane radiator, the maximum distance from the plane where intensity is to be measured must be less than the linear dimensions of the source.

Both point and plane source experiments were performed in a cylindrical tank six feet in diameter and six feet deep filled with water. Measurements of intensity were made by a Geiger-Muller counter encased in a protective aluminum tube (.4 gm/cm^2) and clamped in position at various points along a tank diameter on a metal strip placed across the tank top. In the point source experiment, the source was placed in the tank center and the counter with its axis horizontal was moved along a tank diameter in the plane of the source. Whereas, in the case of the plane, the source was spread out over the bottom of the tank, and the counter with its axis horizontal was moved away from the source.

The counter which had an effective area of 8.8 square inches and was constructed of a one-inch diameter copper tube with .038 inch wall. A five to one ratio of argon to ether mixture at 30 cm of mercury filled the tube, and a five mill tungsten wire served as anode. Rather precise measurements of the counter efficiency (Appendix II and III) were made at three different energies with the results given in the Table of Appendix III. These measurements agree within experimental error of those of Bradt et al[21] so his curve (Figure 5) of counter efficiency is used in all calculations.

Sources used in both experiments were made of Co^{60} which emits a beta ray of 0.3 mev energy and two gamma rays of 1.1 and 1.30 mev, respectively, per disintegration. A Bureau of Standards source contained in a glass ampule and and having an activity of 1.46×10^6 disintegrations per second served as a point source. The plane source was prepared by plating Co^{60} (in the form of $CoSO_4$) in thin copper turnings, measuring the mean activity per gram and spreading this material over a phenolic plane six feet in diameter. This source had an activity of 138 disintegrations per cm^2 per second.

Measurements of background were first taken after

---

[21] H. Bradt, P.C. Gugelot, O. Huber, H. Medicus, P. Preiswerk, and P. Scherrer, "Empfindlichkeit von Zahlrohren mit Beimessing-Aluminumkathode fur -Strahlung im Energieintervall 0.1 Mev Bis 3 Mev", Helv. Phys. Acta 19:77-90, 1946.

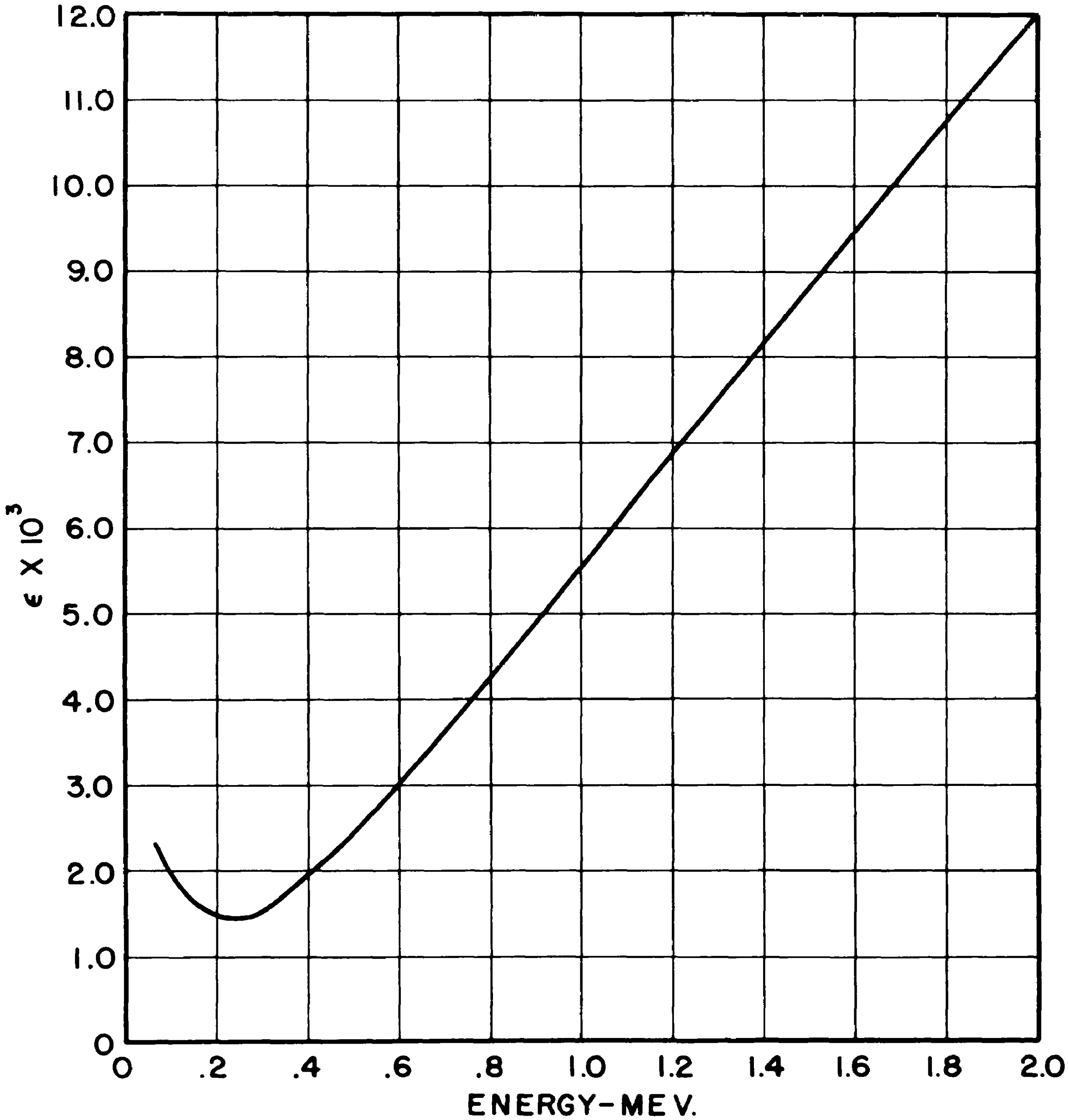

Figure 5. Efficiency of Copper Counter

which the point source was introduced and total counting determinations made at twelve different points along a tank radius. Estimates of the spectral distribution of the quanta were made by a lead shield (2.5 gm/cm^2) placed completely around the counter. Directional data was taken with a thick lead shield of 30 gm/cm^2 mass, surrounding only half the counter; measurements were taken both with the shield facing toward and away from the source. These measurements were repeated with a 2.5 gm/cm^2 lead shield completely surrounding the counters to estimate the energy distribution of the quanta moving toward and away from the source. Transmission coefficients of the various shields and counter tube wall are given in Figure 6 as a function of the energy.

Measurements identical in principal to those above were taken with the plane source. In this case the thin lead shield had a mass per unit area of 1.35 gm/cm^2, while the directional shield had a mass per unit area of 28.7 gm/cm^2.

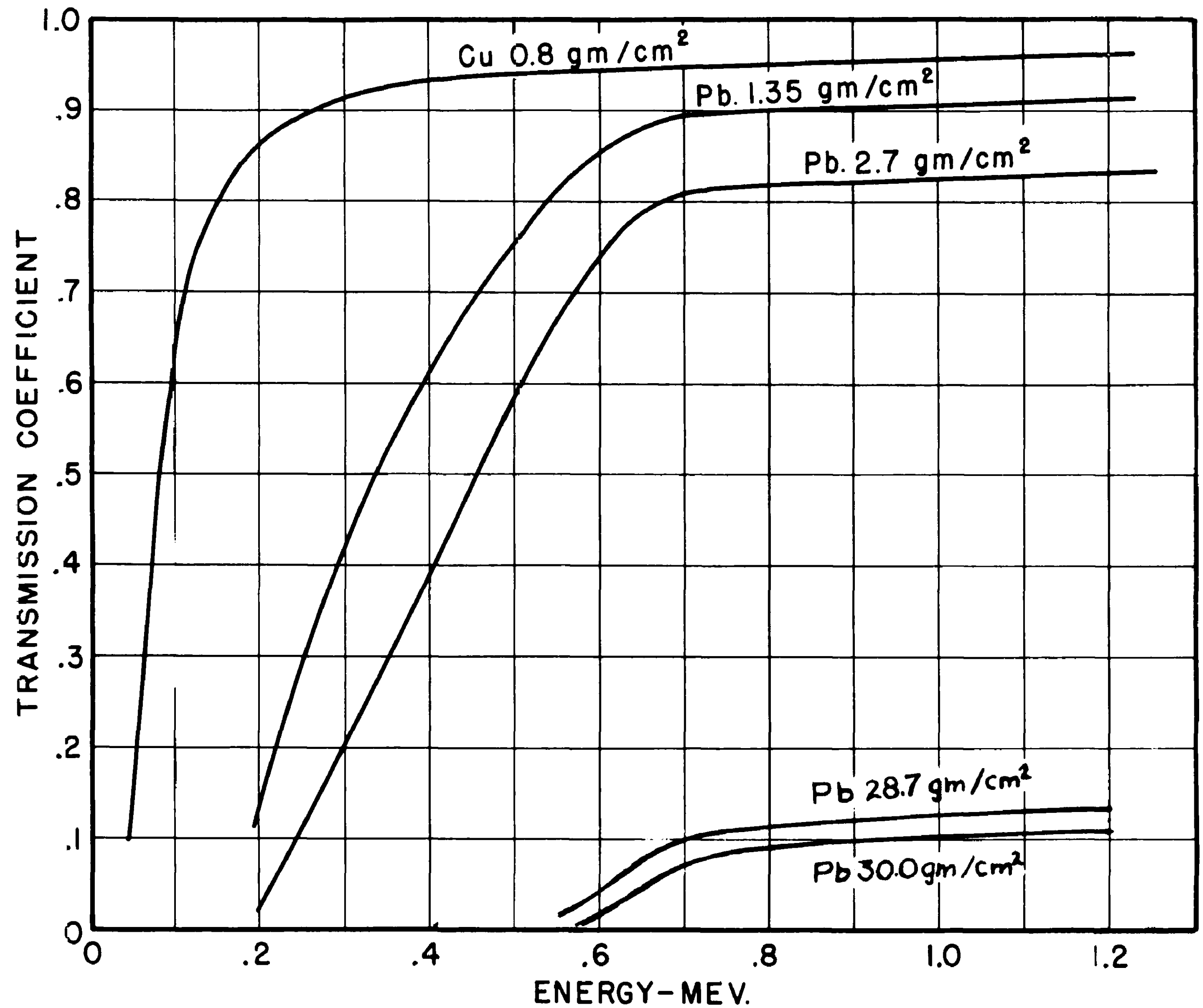

Figure 6. Transmission Coefficients of Shields.

SECTION IV

DISCUSSION OF RESULTS

Counting rates were computed from equations (14) and (22) for the various sources and shields used in the experiment. Results of such calculations are given in Figures 7 to 12 in which experimental data are denoted by circles.

Point source data are compared with the theoretical results in Figures 7, 8, and 9. Figure 7 shows that excellent agreement between theory and experiment was obtained for the unshielded counter while a considerable descrepancy exists in the case of the shielded counter. This descrepancy is due to the use of the mass-absorption coefficient in computing the transmission through the shield. Since the mass-absorption coefficient includes scattering, as well as absorption, its use should over estimate the shielding because quanta scattered in the shield may not be deflected through an angle large enough to miss the counter. The theory, therefore, should be lower than the experimental data in all cases in which a shield is used.

Figure 7 also indicates that the data deviates further from the theory at great distances from the source. This is understandable from the viewpoint that of the quanta which have been scattered, a given number of times, those which have traveled farthest have the largest energy. Thus there are more high energy quanta at distances far from the source than that given by the theory. This effect tends to increase the counting rate but is not so noticeable for the unshielded counter because the efficiency is not directly proportional to the energy; i.e., an increase of group energy below 0.21 mev decreases the counter efficiency which compensates for increases above that value. On the other hand, the counter efficiency is practically linear in the pass-band of the lead filter so that the deviation is more noticeable for the shielded counter.

General agreement of the directional data for the point source with the theory was obtained. Figure 8 indicates that the theoretical curve lies above the data for the negative component and visa versa for the positive component. This is due to the fact that quanta comprising the negative component have been scattered through a larger angle than those in the positive component and, therefore, should have a smaller energy than the positive component. Thus positive and negative components have respectively more and less energy than that calculated by equation (2). Experimental data, therefore, should be displaced in these directions relative to the theory. Further shielding brings out the effects noted previously. First, the larger descrepancy between theory and experiment is due to over estimation of the effect of the shield; and second, the tendency toward higher counting rates far from the source results from a displacement of the group energies toward the high energy end of the spectrum.

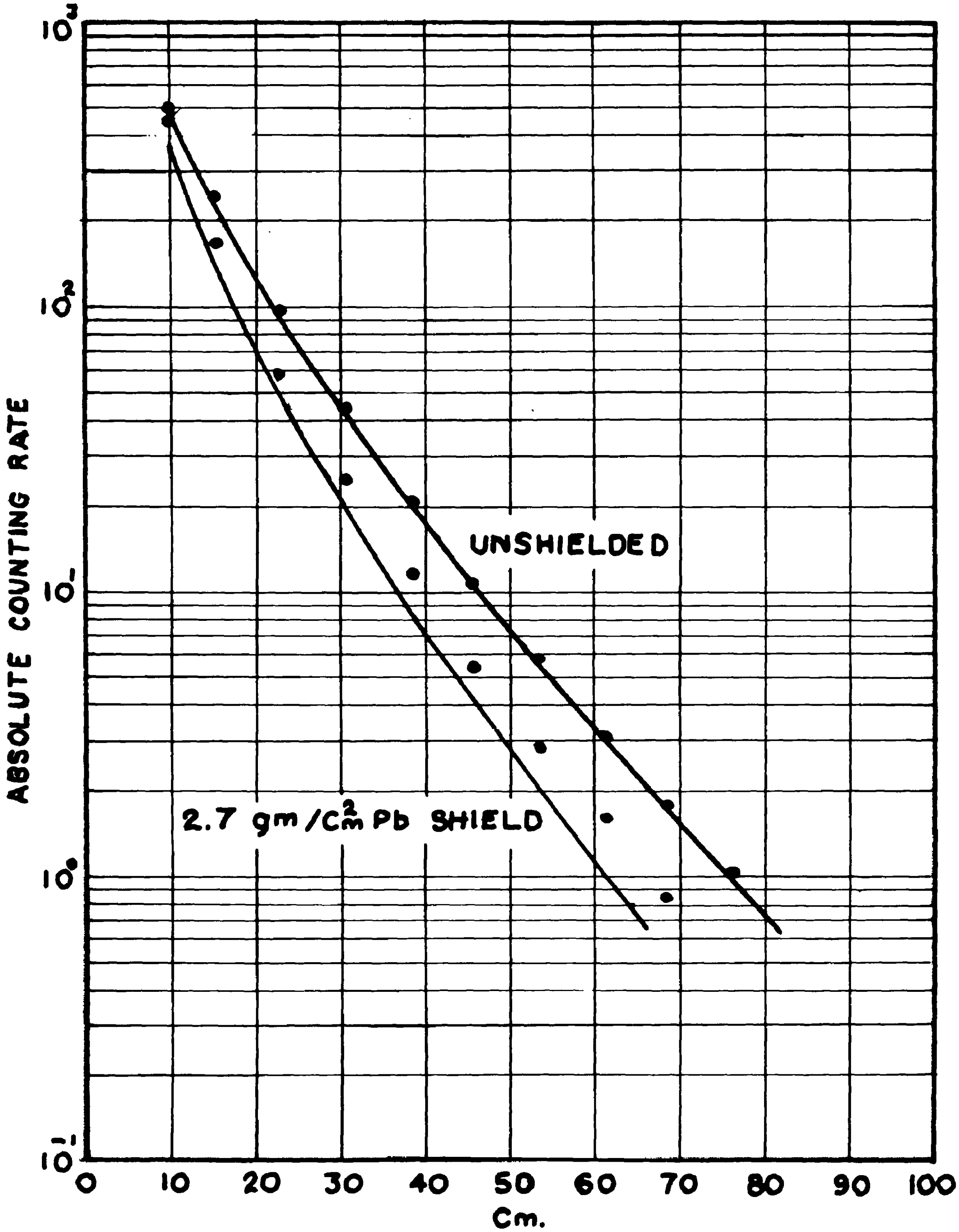

Figure 7. Point Source Counting Rate

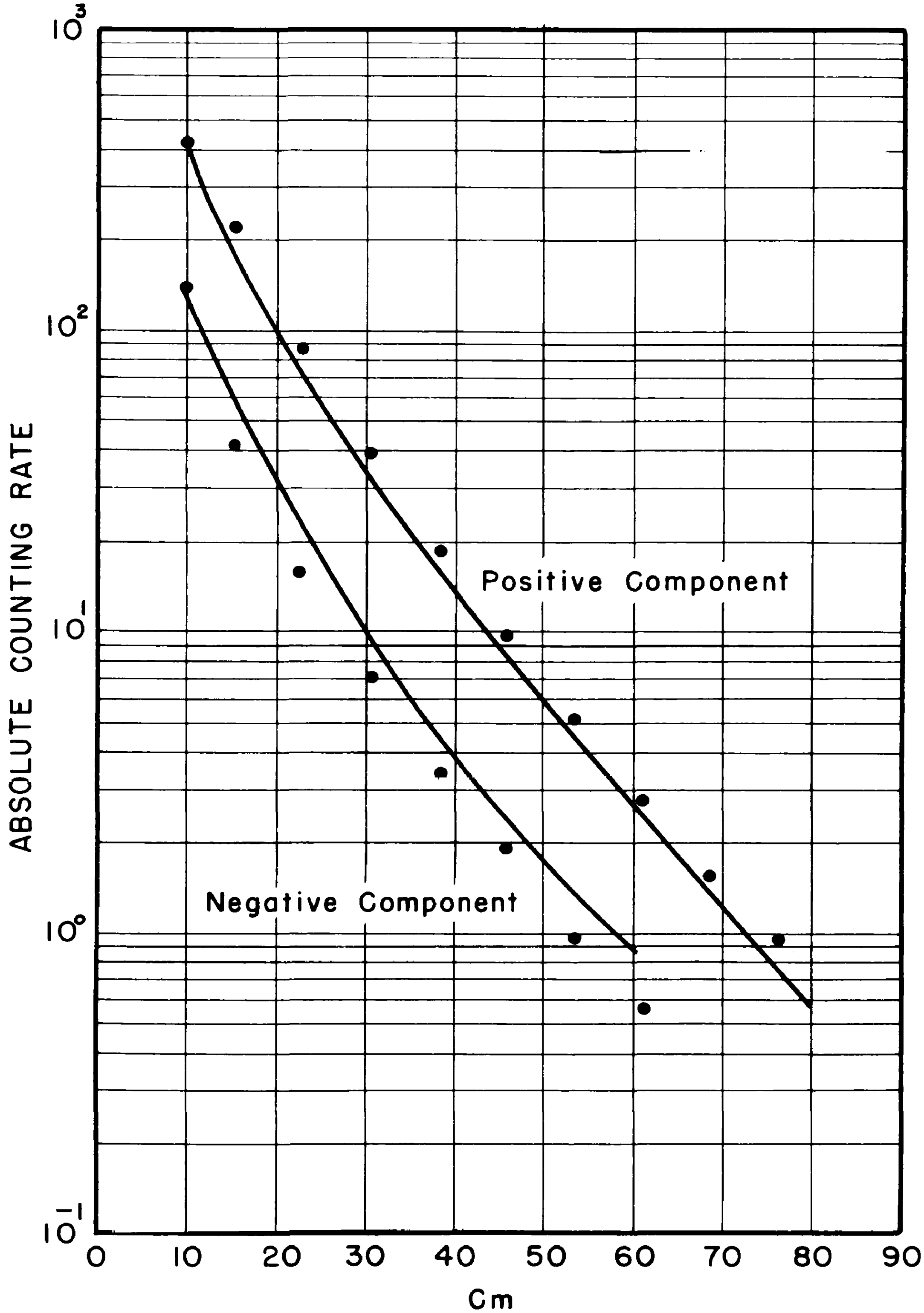

Figure 8. Point Source Directional Counting Rate

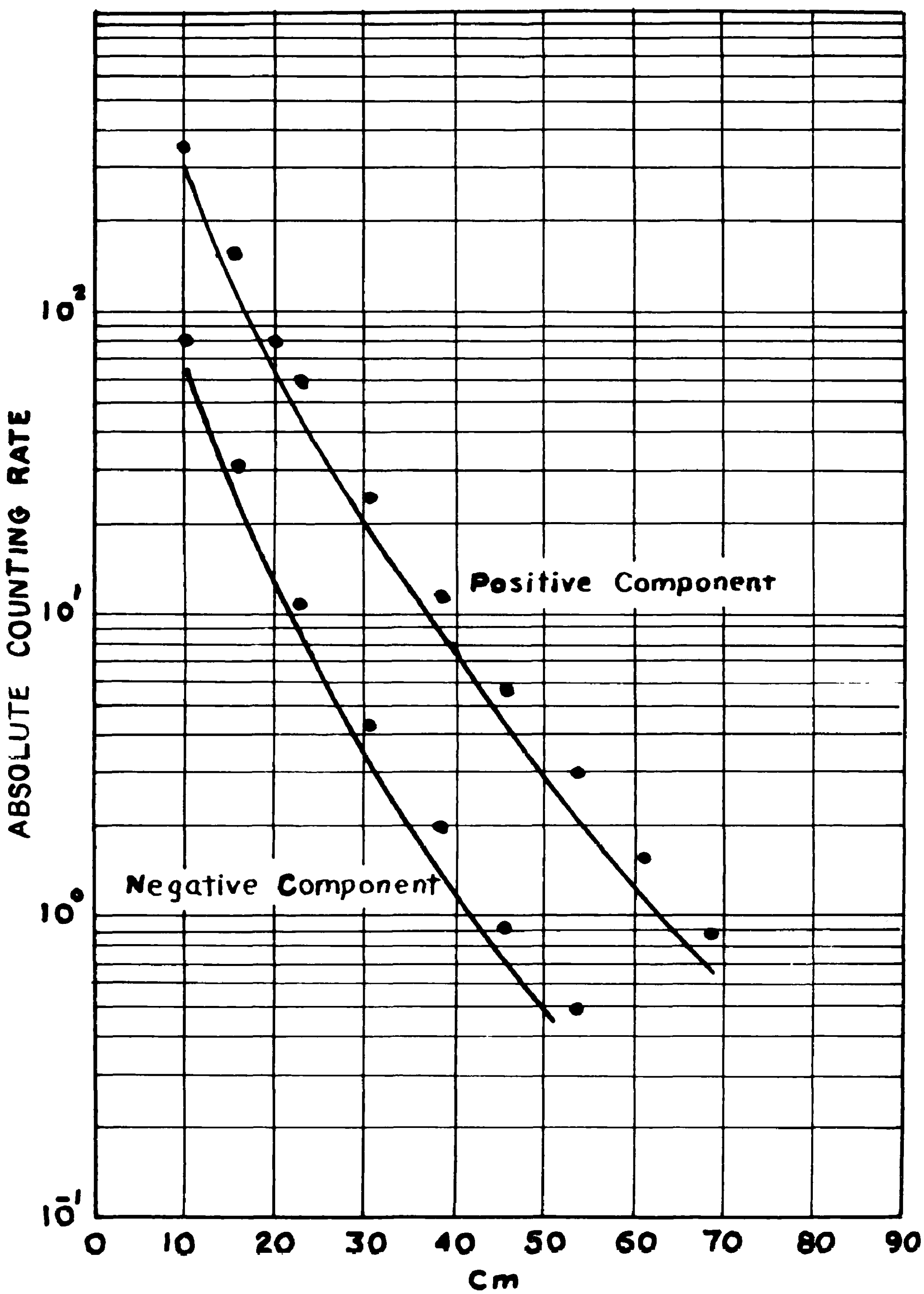

Figure 9. Point Source Directional Counting Rate with 2.5 gm/cm^2 Lead Shield

Comparison between theory and experiment for the plane source is illustrated in Figures 10, 11, and 12. Generally excellent results were obtained for the unshielded counter with experimental error less than two per cent at all points. It is remarkable that this curve beyond 20 cm from the source is exponential with an apparent absorption coefficient of .063 cm^{-1}, which is almost exactly equal to the Compton linear scattering coefficient of .0643 cm^{-1} for water. This is certainly a coincidence as radiation from a plane absorbed with a true absorption coefficient of .0643 cm^{-1} would produce the dotted curve of Figure 10.

Shielding of the counter brings forth the same effects as were observed for the point source. Again, these effects are due to over estimation of the shielding and to a slightly different energy distribution than was assumed in the theory.

Counting rates calculated from the spectral and spatial distribution of the scattered radiation derived in the theory yield results in remarkable agreement with the experimental results. Deviations are easily explicable, although difficult to include in the theory. These distributions, thus, represent a reasonable approximation to the actual distribution and can be used to calculate the radiation under similar conditions.

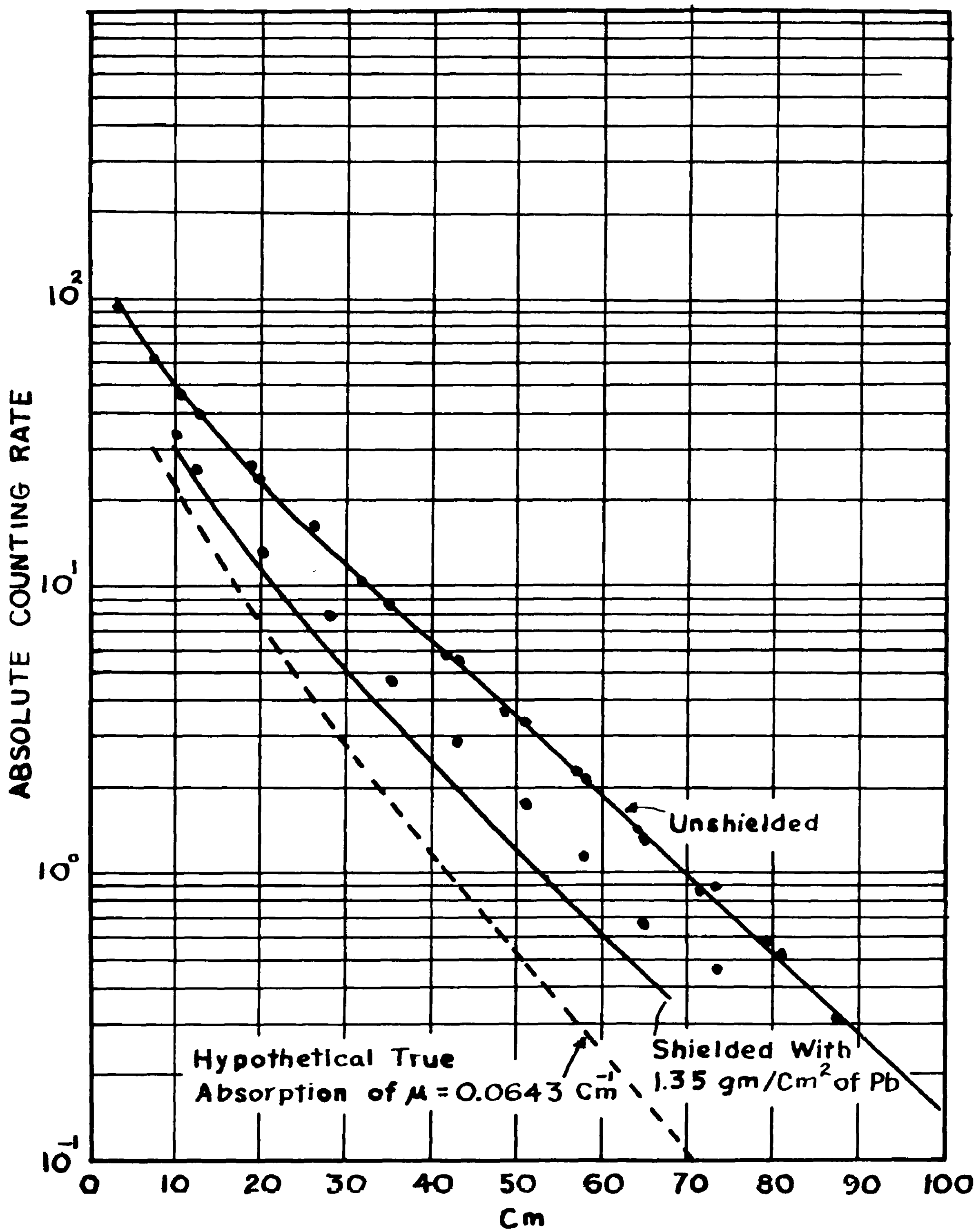

Figure 10. Plane Source Counting Rate

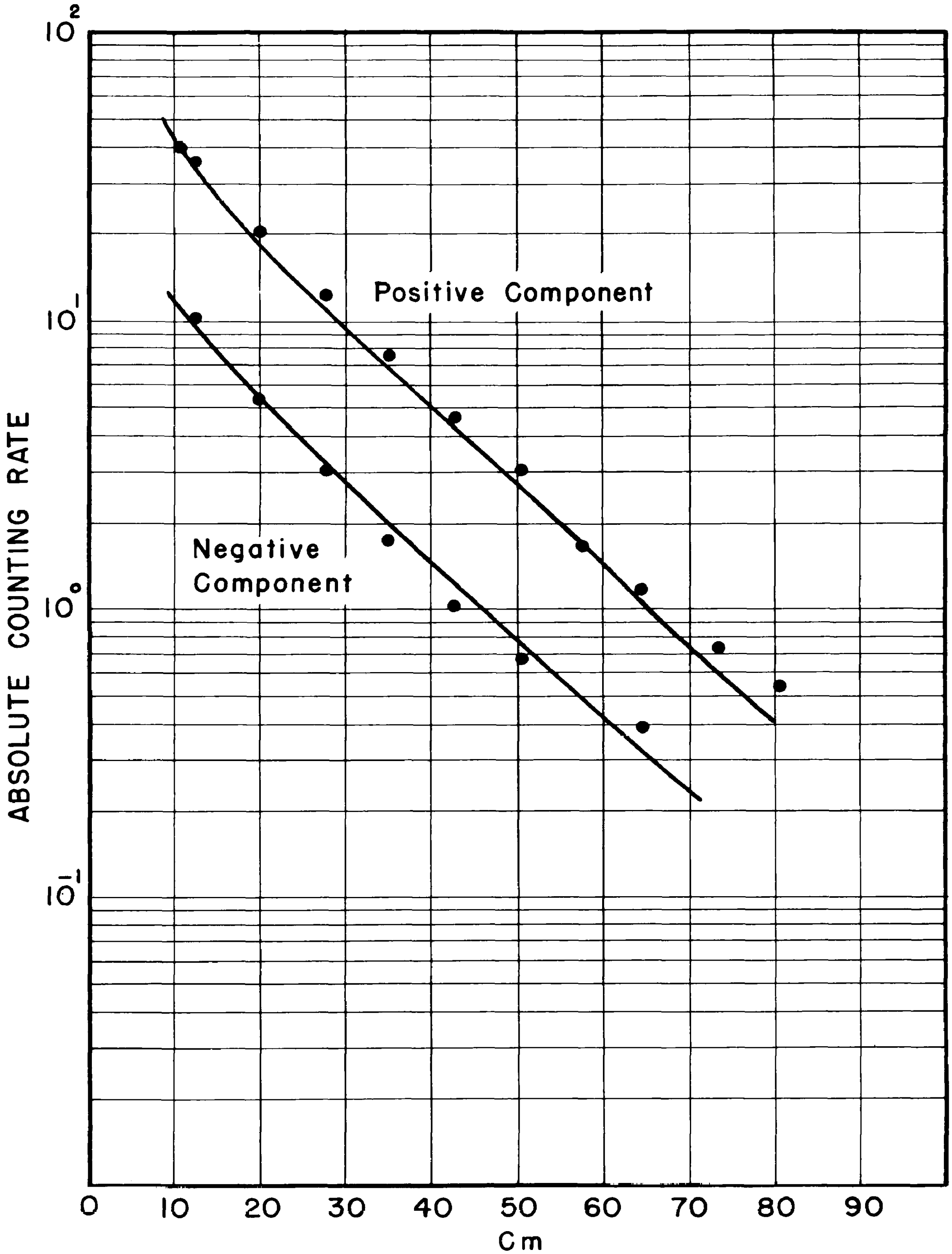

Figure 11. Plane Source Directional Counting Rate

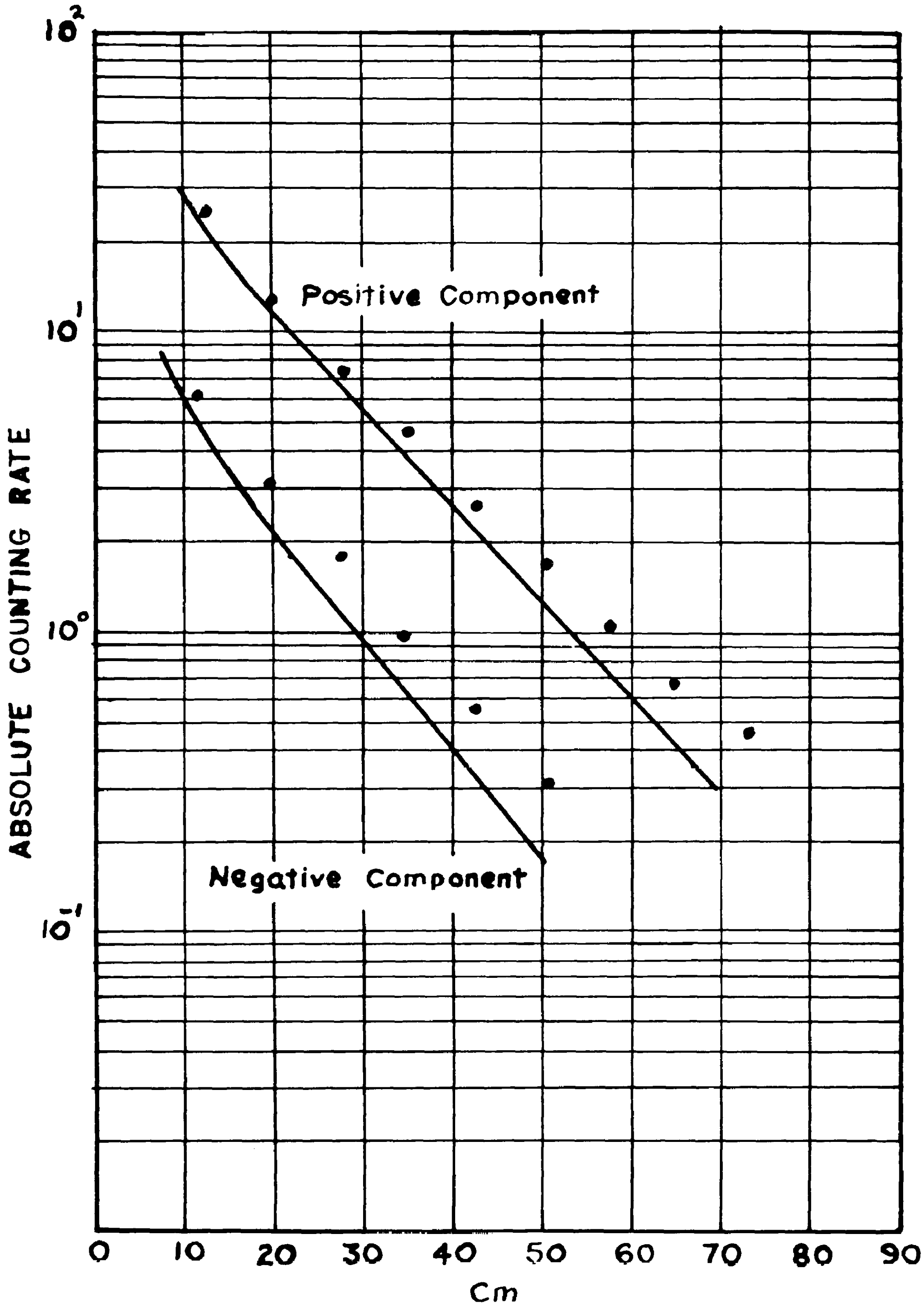

Figure 12. Plane Source Directional Counting Rate with 1.35 gm/cm^2 Lead Shield

APPENDIX I

DISTRIBUTION FUNCTIONS FOR A UNIT POINT SOURCE

(a) $F_o = e^{-\mu_0 Z}$

(b) $F_1^+ = 2.179(e^{-\mu_0 Z} - e^{-\mu_1 Z})$

$F_1^- = 0.1157(e^{-\mu_0 Z})$

(c) $F_2^+ = 3.5610\, e^{-\mu_0 Z} - 8.2640\, e^{-\mu_1 Z} + 4.7030\, e^{-\mu_2 Z}$

$F_2^- = 0.36385\, e^{-\mu_0 Z} - 0.2850\, e^{-\mu_1 Z}$

(d) $F_3^+ = 4.9244\, e^{-\mu_0 Z} - 18.6850\, e^{-\mu_1 Z} - 20.9530\, e^{-\mu_2 Z} - 7.1924\, e^{-\mu_3 Z}$

$F_3^+ = 0.80770\, e^{-\mu_0 Z} - 1.4812\, e^{-\mu_1 Z} - 0.72790\, e^{-\mu_2 Z}$

(4) $F_4^+ = 6.0868\, e^{-\mu_0 Z} - 32.3540\, e^{-\mu_1 Z} - 53.4615\, e^{-\mu_2 Z} - 36.3730\, e^{-\mu_3 Z} + 9.1787\, e^{-\mu_4 Z}$

$F_4^- = 1.3673\, e^{-\mu_0 Z} - 4.1062\, e^{-\mu_1 Z} + 3.9830\, e^{-\mu_2 Z} - 1.2030\, e^{-\mu_3 Z}$

APPENDIX II

Counter efficiency at a given energy can be shown to depend only upon the characteristics of the wall material. Since ionization produced by an electron is essentially independent of the gas characteristics and electron energy, counter efficiency depends only on the relative number of Compton recoils reaching the counter interior. The number of effective recoil electrons formed in volume of the wall, t cm thick of unit area is $N\sigma t$, where t is the maximum range of the electron. From the well known Feather[1] relation

$$t = \frac{1}{d}(.54E - .16)$$

the range t, of an electron varies inversely as the density d. There, counter efficiency is proportional to

$$N \sigma t = \frac{N}{d}(.54E - .6) \sim \frac{Z}{W}(E).$$

where Z and W are respectively the atomic number and weight of the wall material.

---

[1] N. Feather, "Absorption Method of Investigating the High Velocity Limits of Continuous -ray Spectra", <u>Proceedings of Cambridge Philosophical Society</u>, 27: 430-444, August, 1931.

APPENDIX III

A definition of counter efficiency is

$$\epsilon = R/S \tag{1}$$

where R is the counting rate due to the number of quanta, S, incident on the counter persecond. For a counter of effective area A, at a distance l from a source, the number of incident quanta per second is

$$S = \beta n\lambda A/4\pi l^2 \tag{2}$$

where β = Number of quanta emitted per disintegration

$n\lambda$ Activity of source in disintegration per second.

Measurements of counter efficiency were made with Co^{60} and Radium sources with the results given in the table. Excellent agreement was found between these results and those of Bradt.[1]

Efficiency measurements were also made with an x-ray machine at energies of about 0.125 Mev. The counter was placed about one meter from the focus point of the tube and completely shielded in lead except for an aperture of known area. A copper filter was placed between the counter and x-ray machine so that the low frequency part of the spectrum was cut off due to photoelectric absorption in the filter. Intensity measurements were made by a Bureau of Standards

---

[1]H. Bradt, loc. cit.

0.001 Roentgen-Victoreen meter.

In order to calculate the efficiency, the flux of quanta in the beam had to be related to the number of roentgens from the Victoreen meter. Since one r is equivalent to one e.s.u. of change per c.c., the number of ion pairs formed per second is

$$\text{Number of ion pairs per second} = \frac{r/s}{4.8\times10^{-10}} \qquad (3)$$

where r/s is the number of Roentgens delivered per second. It requires 35 volts to form one ion pair in air under standard conditions of pressure and temperatuve so that the energy absorbed per second is

$$\text{Energy/second} = \frac{35 \quad r/s}{4.8\times10^{-10}} \qquad (4)$$

If the quanta producing the ionization have an energy of $h\nu$ (volts), the number of such quanta is

$$\Delta n = \frac{35 \quad r/s}{h\nu \times 4.8\times10^{-10}} \qquad (5)$$

Now as described in the theory, the ratio σ_s/σ is the fraction of incident energy given up to the scattered quantum. $(1 - \sigma_s/\sigma)$ is the energy given to the recoil electron and is the energy effective in producing the ionization. If the x-ray beam has a flux f, the quanta absorbed per cm is μf. The number of quanta effective in producing ionization is $\mu f(1 - \sigma_s/\sigma)$. By substituting this result in Equation (5) it is found that

$$f = \frac{35 \ \Upsilon/s}{h\nu\,(1-\sigma_s/\sigma)\,4.8\times10^{-10}} \tag{6}$$

The efficiency as given by Equation (1) is then

$$\epsilon = \frac{R\ h\nu\ (1-\sigma_s/\sigma)\ 4.8\times10^{-10}}{35A\ \Upsilon/s} \tag{7}$$

where A is the area of the counter tube exposed to the x-ray beam. $(1-\sigma_s/\sigma)$ is evaluated at the energy of the incident quanta.

Results of efficiency measurements with radioactive sources and x-ray machine are given in the following table. Values of Bradt are also given in the table. Agreement of these measurements is excellent.

Source	Mean Energy of γ-Rays	Measured Efficiency	Bradt's Efficiency
Co^{60}	1.20	6.95×10^{-3}	6.8×10^{-3}
Ra	.78	3.8×10^{-3}	3.7×10^{-3}
X Rays	.12	1.4×10^{-3}	1.4×10^{-3}

BIBLIOGRAPHY

1. G.D. Adams, "Absorption of Higher Energy Quanta", *Physical Review*, 74: 1702-1712, October, 1948.

2. S. Chandrasekhar, "The Softening of Radiation by Multiple Compton Scattering", *Proceedings of the Royal Society*, 192: 508-518, March 18, 1948.

3. A.H. Compton and S.K. Allison, *X Rays in Theory and Experiment* (New York, D. Van Nostrand, 1935) Chap. III, pp. 116-262.

4. H. Bradt, P.C. Gugelot, O. Huber, H. Medicus, P. Preiswerk, and P. Scherrer, "Empfindlichkeit von zahlrohren mit Beimessing-Aluminumkathode fur -Strahlung im Energieintervall 0.1 Mev Bis 3 Mev", *Helv. Phys.* Acta 19: 77-90, 1946.

5. W.R. Faust and M.H. Johnson, "Multiple Compton Scattering", *Phy. Rev.*, 75: 467-472, February, 1949.

6. N. Feather, "Absorption Method of Investigating the High Velocity Limits of Continuous -ray Spectra", *Proceedings of Cambridge Philosophical Society*, 27: 430-444, August, 1931.

7. W. Heitler, *Quantum Theory of Radiation* (Oxford, Cambridge, 1944), pp. 129-137.

8. J.O. Hirschfelder, J.L. Magee, and M.H. Hull, "Penetration of Gamma Radiation through Thick Layers", *Phy. Rev.*, 73: 852-868, April 15, 1948.

9. E. Hopf, *Problems of Radiative Equilibrium* (Oxford, Cambridge, 1932), pp. 2-12.

10. H.R. Hulme, J. McDougall, R.A. Buckingham, and R.H. Fowler, "The Photoelectric Absorption of rays in Heavy Elements", *Proceedings of the Royal Society*, 194: 131-151, January, 1935.

11. Eugene Jahnke and Fritz Emde, *Tables of Functions*, (New York, Dover Publications, 1945), pp. 6-9.

12. G.E.M. Jauncy and G.G. Harry, "The Scattering of Unpolarized X Rays", *Phy. Rev.*, 37: 698-711, May, 1931.

13. O. Klein and Y. Nishima, "Uber die Streuung Von Strahlung durch freie Electronen nach der neuen relativistichen Quantemdynamik Von Dirac", *Zeitschrieft fur Physik*, 52: 853-868, May, 1929.

14. L.F. Lamerton, "Theoretical Study of Results of Ionization Measurements in Water with X rays and Gamma Rays", British Journal of Radiation, 1: 246, June, 1948.

15. L. Meitner and H. Upfeld, "Uber das Absorptionsgesetz fur Kurzwellige -struhlung", Zs. f. Phys., 67: 147-168, February, 1931.

16. J.R. Oppenheimer and M.S. Plesset, "On the Production of the Positive Electron", Phy. Rev., 44: 53-55, January, 1933.